Bio-inspired swing leg control for spring-mass robots running on ground with unexpected height disturbance

2013 Bioinspir. Biomim. 8 046006

(http://iopscience.iop.org/1748-3190/8/4/046006)

IOP Publishing Bioinspiration & Biomimetics
Bioinspir. Biomim. **8** (2013) 046006 (13pp) doi:10.1088/1748-3182/8/4/046006

Bio-inspired swing leg control for spring-mass robots running on ground with unexpected height disturbance

H R Vejdani[1], Y Blum[2], M A Daley[2] and J W Hurst[1]

[1] Dynamic Robotics Laboratory, Oregon State University, Oregon, USA
[2] Structure and Motion Laboratory, Royal Veterinary College, Hertfordshire, UK

E-mail: hrvn@engr.oregonstate.edu

Received 27 March 2013
Accepted for publication 3 October 2013
Published 29 October 2013
Online at stacks.iop.org/BB/8/046006

Abstract
We proposed three swing leg control policies for spring-mass running robots, inspired by experimental data from our recent collaborative work on ground running birds. Previous investigations suggest that animals may prioritize injury avoidance and/or efficiency as their objective function during running rather than maintaining limit-cycle stability. Therefore, in this study we targeted structural capacity (maximum leg force to avoid damage) and efficiency as the main goals for our control policies, since these objective functions are crucial to reduce motor size and structure weight. Each proposed policy controls the leg angle as a function of time during flight phase such that its objective function during the subsequent stance phase is regulated. The three objective functions that are regulated in the control policies are (i) the leg peak force, (ii) the axial impulse, and (iii) the leg actuator work. It should be noted that each control policy regulates one single objective function. Surprisingly, all three swing leg control policies result in nearly identical subsequent stance phase dynamics. This implies that the implementation of any of the proposed control policies would satisfy both goals (damage avoidance and efficiency) at once. Furthermore, all three control policies require a surprisingly simple leg angle adjustment: leg retraction with constant angular acceleration.

(Some figures may appear in colour only in the online journal)

1. Introduction

We seek to understand the principles of legged locomotion and to implement them on robots. Recent years have seen remarkable advances in dynamic legged robots, including Rhex, a rough-terrain hexapod [1, 2], Bigdog, a rough terrain quadruped [3], MABEL, a biped that can negotiate uneven terrain [4], ATRIAS, a bio-inspired actuated spring-mass robot [5], and PETMAN, a versatile humanoid biped. These robots highlight the emerging potential for legged robotic technology; however, none of these machines can compete with animal performance and efficiency. In natural environments animals frequently negotiate potholes, steps and obstacles remarkably, while running. Because we do not yet understand the fundamental principles of locomotion that enable such performance, we cannot reproduce these behaviors in machines [6]. In this study we seek to identify reasonable objective functions animals might care about, and use them to control a spring-mass running robot. To gain insight into the goals birds may care about during running, we investigated guinea fowl running data (figure 1) and interpreted the importance of those goals for real machines.

There are two reasons why we focus on swing leg control: (i) the flight phase determines the landing conditions, which have huge effects on stance dynamics, and (ii) adjusting the leg parameters during flight is very energy efficient because there are no ground reaction forces to overcome during flight to move the leg. The effect of swing leg control methods on the dynamics of a spring-mass system has been investigated in previous literature [8–12]. From a biologist's perspective, animal running data reveal that the initial leg loading during stance is very sensitive to its landing conditions, which are

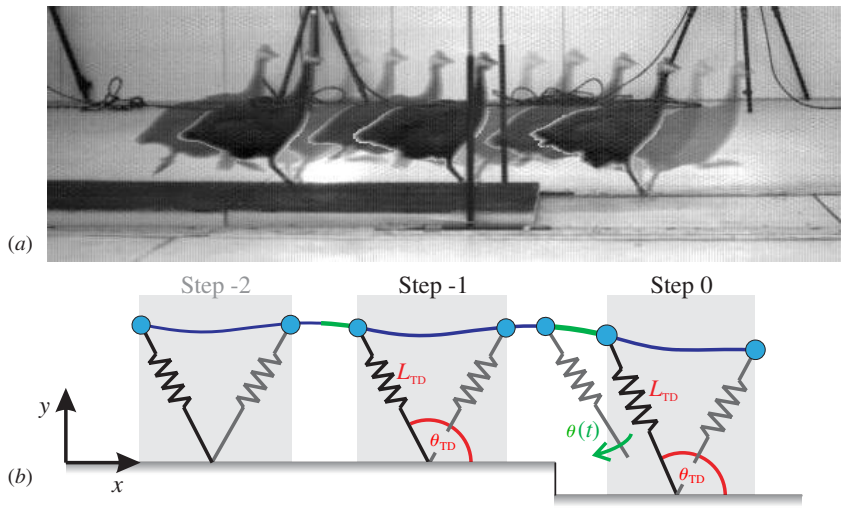

Figure 1. Illustration of experiment setup on the guinea fowl running over a step down (*a*), and schematic drawing of the SLIP model (*b*). The gray areas indicate the stance phases, and the blue line represents the CoM trajectory [7].

determined by the flight phase [13–16]. Daley *et al* [17] showed that for running guinea fowl, the variation in leg contact angles explains 80% of the variation in stance impulse after an unexpected pothole. From a roboticist's point of view, using a feed-forward control strategy minimizes the need for sensing, which makes these techniques easy to implement in robots.

Previous theoretical studies of swing leg control suggest a trade-off between objectives like disturbance rejection, stability, maximum leg force and impact losses. For example, a constant leg retraction velocity in late swing improves stability in both quadrupeds [18] and bipeds [10]. Similarly, increasing the leg length in late swing can improve stability and robustness [11]. Whereas low leg retraction velocities improve the robustness against variations in terrain height, high leg retraction velocities minimize peak forces and improve ground speed matching [19, 20]. Alternatively, a feed-forward swing leg control policy can be applied to the spring-loaded inverted pendulum (SLIP) model to maintain steady state running (equilibrium gait), regardless of ground height changes [21]. While maintaining steady state running results in symmetric trajectories even in the presence of ground height changes, it also results in high leg forces and high leg actuator work (electric consumption of the electric motor) during the perturbed step. Karssen *et al* [22] determined the optimal swing leg retraction rate that maximizes disturbance rejection, and minimizes impact losses and foot slipping. They considered a pre-defined constant leg retraction rate for running and concluded that there exists no unique retraction rate that optimizes all goals mentioned above at the same time. Especially for high forward speeds, a compromise between disturbance rejection and energy losses is inevitable. Recently, Ernst *et al* [12] demonstrated how leg stiffness may affect the self-stability of a running robot. They proposed a control strategy that updates the leg stiffness based on the fall time or vertical velocity of the center of mass (CoM).

The equilibrium (symmetric) gait policy is a well-investigated swing leg control policy for spring-mass robots [12, 21]. This policy ensures that the robot's CoM trajectory is symmetric with respect to the vertical axis, which is defined by mid-stance (touch-down and take-off conditions are symmetrical). Therefore, on flat ground each step is identical to the previous step, resulting in a periodic gait pattern. By choosing the appropriate initial leg angle (touch-down leg angle) for each velocity vector $\boldsymbol{v} = (v_x, v_y)^T$, a symmetric gait can be obtained. This policy continuously updates the leg angle based on the CoM velocity vector during flight such that whenever the leg hits the ground, a symmetric CoM trajectory is maintained. In the presence of a drop, however, the required mechanical capacity (leg force for example) can increase drastically, and may exceed the ultimate leg capacity. Therefore, the equilibrium gait policy may not be a practical control strategy for spring-mass robots.

Inspired by our findings from a previous study on guinea fowl negotiating a drop perturbation [7], we propose three candidates for the objective function of the swing leg control policy. The objective functions are: (i) maintaining constant peak force, (ii) maintaining constant leg axial impulse, and (iii) maintaining constant leg actuator work. Each control policy adjusts the leg angle during flight such that its objective function during the subsequent stance phase is regulated. The first swing leg control policy ensures that the leg peak force in the following stance phase is the same as the peak force of the previous step. The second policy keeps the axial impulse of the upcoming passive stance phase the same as the axial impulse of the previous step. The last control policy focuses on economy by maintaining constant electrical work to keep the motor, which is in series with the spring, locked (providing zero mechanical work and thus a conservative passive stance phase). In this case the actuator requires the same electric energy for the drop step and flat ground. We compare these control policies with equilibrium gait policy and against each other.

The results show that the equilibrium gait policy requires more energy and leg force capacity than the proposed control policies. For economically designed robots that are operating at (or close to) their maximum mechanical capacity, any drop in the ground may cause damage, or the robot could even fall if the motors are not strong enough. Moreover, it turns

out that with a simple swing leg control policy, retracting the leg with constant angular acceleration, both goals (optimizing mechanical demand and energy efficiency) could be met at once.

2. Bioinspiration

We are inspired by the robust and efficient running of animals. Guinea fowl, for example, locomote highly agile, robust and efficient in natural environments (uneven terrain). We want to identify control policies that make running legged robots perform as proficiently as animals like guinea fowl.

Our strategy is to exploit results from experiments that have been conducted by Blum *et al* [7] on guinea fowl negotiating a drop perturbation, and hypothesize policies these birds may follow during running. The experimental setup they used is shown in figure 1.

The results suggest that the leg touch-down angle may be the main parameter that guinea fowl control during flight phase. Furthermore, force data show that leg peak forces and axial impulses are nearly constant during level running and in the presence of a drop [7].

3. Methods

In this section we describe the model that we use in this study and our proposed control policies. We use the SLIP model (section 3.1) as the model for our running robot, and our hypothesized control policies (section 3.2) will be applied on this model during running. We assume the system is running on level ground and without any prior information, an unknown disturbance in the ground occurs. Each control policy regulates an objective function (section 3.2) to handle the disturbance. We focus on step-down disturbances through all of our simulations because the only challenge for step-up disturbances is a geometric constraint between the toe and the ground that may lead to a stumble or a fall. Once the geometric constraint for step-up disturbances is solved (by changing the length of the swing leg and adjusting the leg angle accordingly), an equilibrium gait can be obtained without suffering leg force or work increase. We will discuss this case more in stability analysis section (section 5.1) and in the discussion section as well.

3.1. Model

We consider the SLIP [23, 24], because the passive model of the spring-mass robot is similar to the SLIP model. The SLIP model is a well-known template for studying legged locomotion [25]. This model is based on the ubiquitous CoM trajectory that animals have during running. Both humans and birds can deviate from SLIP dynamics for very large disturbances; yet, numerous studies [9, 11, 13, 26–29] have investigated human locomotion in response to terrain perturbations and found that humans follow SLIP like behavior for a range of disturbances. It should be noted that animals and actual spring-mass running robots have leg actuators in series with a spring (figure 2) to compensate for the energy loss due to friction and impacts. However, the mechanical energy generated/dissipated by the motor is low, and thus the system can be accounted as a passive conservative SLIP model. Because the model is passive during stance phase we do not need the leg motor in our simulation, but its existence cannot be ignored. Therefore, we keep the leg motor locked (zero mechanical work) to have a conservative system (SLIP-like) and consider a criteria for the required electric energy.

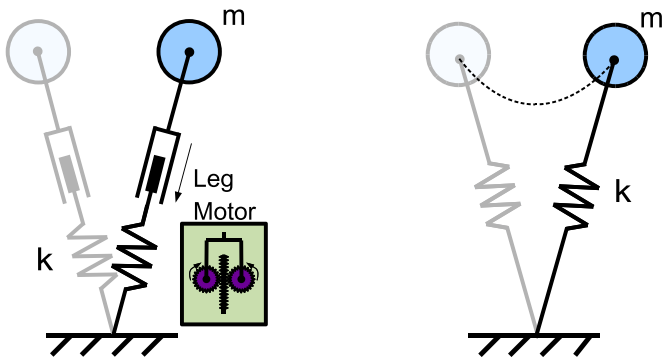

Figure 2. Left: the model of the robot with the leg motor. The reason of the leg motor existence is to add energy into the system when some energy is lost due to impact or friction. Here, this motor is kept locked (zero mechanical energy) to provide the equivalent conservative SLIP model that is shown in the right.

Table 1. Properties of the spring-mass robot.

Parameter	Description	Value
m	Robot mass	38.0 kg
k_{leg}	Leg spring stiffness	3900 N m^{-1}
v_{0x}	Initial horizontal velocity	3.5 m s^{-1}
h_0	Initial CoM height	57 cm
δ_{gnd}	Ground disturbance	−10 cm

During flight phase of running the CoM describes a ballistic curve, determined by the gravitational force. Therefore, the only leg parameters that can be controlled during the flight phase are the landing conditions for the upcoming stance phase. The transition from flight to stance occurs when the landing condition $y = L_0 \sin(\theta_{\text{TD}})$ is fulfilled. During stance phase the equation of motion for a passive SLIP model is given by

$$m\ddot{\boldsymbol{r}} = k_{\text{Leg}}\left(\frac{L_0}{r} - 1\right)\boldsymbol{r} - m\boldsymbol{g},$$

with $\boldsymbol{r} = (x, y)^T$ being the position of the point mass with respect to the foot point, r its absolute value and $\boldsymbol{g} = (0, g)^T$ the gravitational acceleration, with $g = 9.81\text{m}\,\text{s}^{-2}$. Take-off occurs when the spring deflection returns to zero. The system is energetically conservative and due to the massless leg there are no impact or friction losses in the system.

The model was implemented in Matlab (R2012a, Mathworks Inc., Natick, MA, USA). To accomplish the simulations, following properties for the robot (table 1) were assumed.

3.2. Proposed control strategies

Inspired by the running behavior of birds mentioned in section 2, we propose three swing leg control policies. We focus on flight phase control policies because, contrary to stance control, we can theoretically do no work and still control the gait. Therefore, the controllers are economically efficient. Leg angle during flight is the only parameter that is changed in all three proposed control policies. Each policy controls the trajectory of the leg angle as a function of time $\theta(t)$ (or vertical velocity) such that its objective function is regulated in the upcoming passive stance phase. The objective function for each policy is (i) the leg peak force, (ii) the axial impulse, or (iii) the leg actuator electric work. Therefore, each control policy adjusts the leg angle during flight at each instant to keep its objective function the same as in the previous step. When there is no ground height disturbance (level running), all control policies result in equilibrium gait.

We assume that our model has no information about the location and the size of the drop perturbation, and the leg angle is adjusted continuously starting at the instant of the expected touch-down in anticipation of ground contact. Therefore, on flat ground, equilibrium gait is obtained. In the presence of a drop, however, the leg angle is adjusted at each instant such that the objective function is regulated in the subsequent stance phase. It should be noted that no control is applied during stance, which is purely passive.

3.2.1. Constant peak force policy. The first proposed control strategy is to regulate the peak force during running. The constant leg peak force control policy adjusts the leg angle during flight such that the resulting leg peak force during stance of any drop step remains the same as for level running. This control policy allows for running robots to operate at their maximum capacity on even terrain and relinquishes the need to reserve some of the mechanical capacity, motor torque and structural strength for the drop step, and hence yields to lighter and more efficient robots. Experimental data show that running birds maintain nearly constant peak forces during running and in the presence of a drop ([7]). It should be noted that the controller does not need any information about the size and location of the drop (minimal sensing), since the leg angle is adjusted continuously during the flight phase such that the leg peak force gets regulated.

In the presence of a drop, the leg angle retracts towards the ground. Contrary to equilibrium gait policy, as indicated in the appendix, constant peak force policy always retracts the leg to fulfil its objective function. This behavior helps to reach the ground sooner and hence prevents the vertical velocity from increasing further. The reason that the leg is retracted before hitting the ground in this control policy is as follows: as the robot falls, the vertical velocity of the CoM increases and consequently the velocity vector rotates towards the leg. To avoid an increase of the peak force, the angle between the velocity vector and the leg direction needs to be increased. To increase this angle, the leg has to be retracted even faster than the rotation of the velocity vector toward the leg.

3.2.2. Constant axial impulse policy. The axial impulse is another objective function that we propose to be regulated during running. We chose the axial impulse, because this function considers both leg force and leg work at the same time (our two goals), maintains consistent energy storage in the spring, and is also able to reproduce the observed animal behavior. The constant leg impulse control policy provides the same axial impulse for the drop step as during level running by adjusting the leg angle during flight. This control policy—like the constant peak force control policy—retracts the leg at the presence of a drop perturbation, regulating the axial impulse to be the same as during level running.

The mathematical formula for the axial impulse is:

$$I = \int_0^{t_s} F \, \mathrm{d}t,$$

where, F is the force in leg direction and t_s the stance time.

3.2.3. Constant leg work policy. Our third proposed control policy, constant leg work policy, directly targets the efficiency of the system. The motivation for this objective function comes from observation from animals running on natural environment and still they are very efficient.

It should be noted that the connection of muscles and tendons in animals is similar to the connection of a motor in series with a leg spring for running robots. Although the whole system remains energetically conservative and the generated/dissipated mechanical work is zero, the leg actuator requires electric energy to hold a fixed position.

To regulate the electric work for this control policy in the drop step, the leg angle is adjusted such that the electric energy of the leg actuator is the same as for level running. The consumed electric energy to keep the motor locked during the stance phase is the integral of the power over time

$$EW = \int_0^{t_s} \|P\| \, \mathrm{d}t.$$

Since the power in the electric motors is equal to $P = V \cdot I$, and $V = R \cdot I$, by considering the relation between the torque and current in electric motors, the required electric energy can be obtained. It should be noted that from the robotics point of view, when negative mechanical work is generated, it should be treated differently because of the energy loss in the system. Since in this study the leg motor is kept locked during the stance phase, no negative work is produced. Therefore the consumed electrical energy is proportional to the integral of the torque squared over stance time. We use this integral as the criteria for the actuator electric work. The mathematical formula for this criteria is defined as the following function which has been used as the cost function for optimization problems in other studies [30–32]:

$$W = \int_0^{t_s} F^2 \, \mathrm{d}t.$$

Here, W is the work criteria that is proportional to the consumed electric energy to keep the leg motor locked. The leg force is shown by F and the stance time is t_s. This control policy that regulated the actuator electric energy—like the two previous control policies—retracts the leg in the presence of a

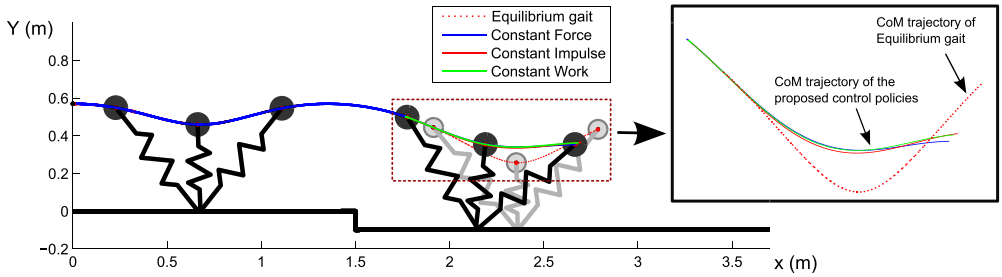

Figure 3. CoM trajectories of the robot subjected to the three proposed control policies and equilibrium gait control policy. For the proposed control policies the height of the CoM is lower at take-off respect to touch-down and equilibrium which implies that the system would have higher forward speed at take-off. This is the same behavior that we observe from animals.

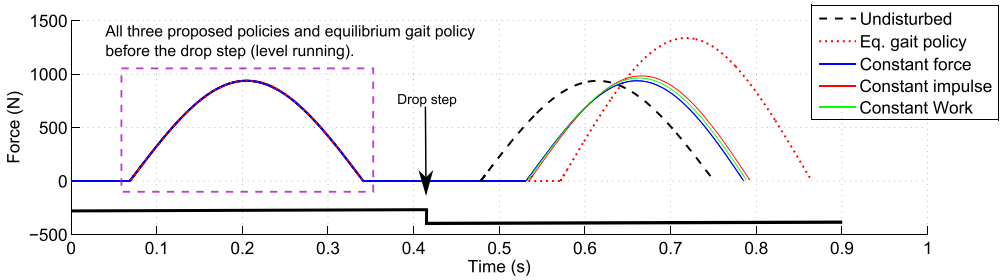

Figure 4. Axial force profiles for the three proposed control policies and the equilibrium gait control policy and undisturbed situation. The peak force in equilibrium gait control policy increases about 45% respect to the undisturbed peak force. The beginning of the force profiles show that the equilibrium gait policy reaches the ground the last.

drop to keep the leg actuator work constant and consequently, like before, the leg reaches the ground sooner because of the steeper leg angle at the time of the touch-down. It should be noted that the required energy for the swing leg is not significant because the SLIP model has a massless leg (and hence the robots that are designed based on this model have very light legs and the motors to move these light legs have small inertias), and consequently no force and energy are needed for the leg rotation (or very small for real world robots).

4. Results

In this section we investigate, in simulation, the success of the control policies in the presence of a hidden drop step, and then compare the three proposed control policies against the equilibrium gait policy (see appendix) and against each other. Since the system follows its passive dynamics during stance, the difference in the behavior of the system for each policy comes only from the different touch-down angles.

As figure 3 shows, the overall shape of the CoM trajectories during the drop step are very similar for the three proposed control policies and clearly different from the equilibrium gait policy. In this figure the CoM trajectories of the step before the drop and the drop step itself are shown. Because the robot does not have any information about the disturbed step, the step before the drop is the identical to level running. All three control policies could successfully pass the drop step, and the robot did not fall. The constant force control policy causes the model to touch the ground slightly sooner than the other two policies, and hence results in a lower CoM height and less vertical velocity.

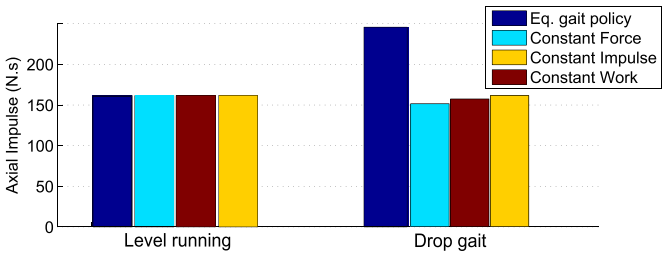

Figure 5. Axial impulse in the leg during the stance phase for level ground and drop step. The axial impulse for drop step with equilibrium gait control policy is much higher than the level running. For the constant peak force and constant work policies, the axial impulse in drop step decreases a little bit respect to the level running.

The CoM trajectories in figure 3 imply that the robot accelerates horizontally in the drop step for all three of the proposed control policies, while for equilibrium gait policy the robot maintains the same forward speed as before. It should be noted that, although part of the potential energy of the system is redirected into horizontal kinetic energy, since the velocity contributes quadratically to kinetic energy, the resulting horizontal velocity after take-off does not increase drastically.

The leg force profiles are shown in figure 4. The leg peak force in the drop step for equilibrium gait policy increases by 45% compared to level running, while for the proposed control policies it remains nearly constant. For both constant impulse and constant work policy, the leg peak force increases slightly.

The axial impulse decreases slightly in the drop step for both constant peak force and constant actuator work policy (figure 5), but increases by 60% for equilibrium gait policy.

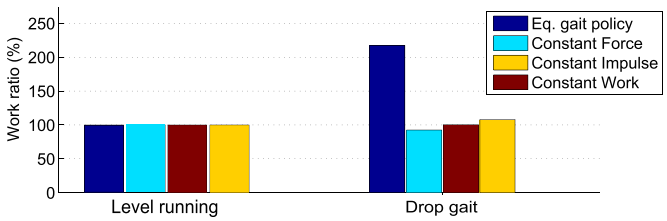

Figure 6. Actuator electric work criteria to keep the motor locked during the stance phase. The required work for drop step with equilibrium gait control policy is much higher than the level running (more than two times), but the required electric work with constant peak force control policy is nearly the same as level running.

Figure 6 compares the efficiency of the control polices based on required electric energy. The constant axial impulse policy requires 7% more electric work for the drop step than during level running, while the constant peak force policy needs the least electric energy in the drop step (about 5% less than during level running). Whereas the proposed control policies require nearly the same amount of electric energy in the drop step as during level running, the required electric energy for the equilibrium gait policy in the drop step is more than 200% of what is required for level running.

Figure 7 shows that the general behavior of the system with the proposed control policies is consistent for different leg stiffness and drop heights. The system can recover from higher drop heights when the leg stiffness is greater, which means the robustness of the system increases for these control policies with increasing the leg stiffness. For the peak force control policy, as an example, the CoM trajectory trends of the system for different drop heights are shown in figure 8.

A comparison of the touch-down angles for each control policy is shown in figure 9. This figure qualitatively illustrates how the control policies choose leg angles through a range of vertical velocities. In this figure the proposed control policies are depicted in the peak force, impulse and leg work contour lines. Moving along each contour line means following the corresponding control policy. During level running, all three proposed control policies and the equilibrium gait policy exhibit the same behavior, illustrated by the gray big circle in the figure. The small colored circles show the touch-down conditions of the robot following each of the control policies in the drop step. As the vertical velocity increases, the contour lines diverge from each other, which implies a more different behavior of the system for each control policy in larger drops.

The shapes of the contour lines in figure 9 are nearly linear for small changes in vertical velocity. To study the shape of the contour lines further, we focus on only on the peak force contour lines, shown in figure 10. This figure shows the desired leg angle trajectory, which is a peak force contour line, and two fits (linear and quadratic function) for the desired leg angle trajectory. The linear fit of the desired leg angle trajectory drifts along the desired curve, and this drift gets smaller with

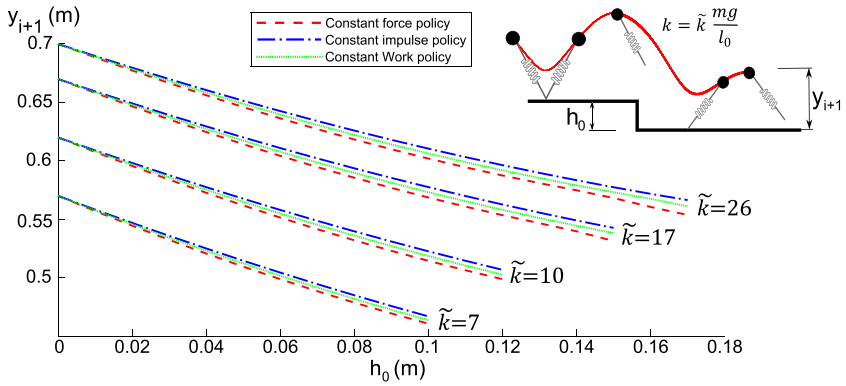

Figure 7. The effect of the leg stiffness and drop height on the behavior of the system with the proposed control policies. The behavior of the system is consistent for different leg stiffness and drop heights.

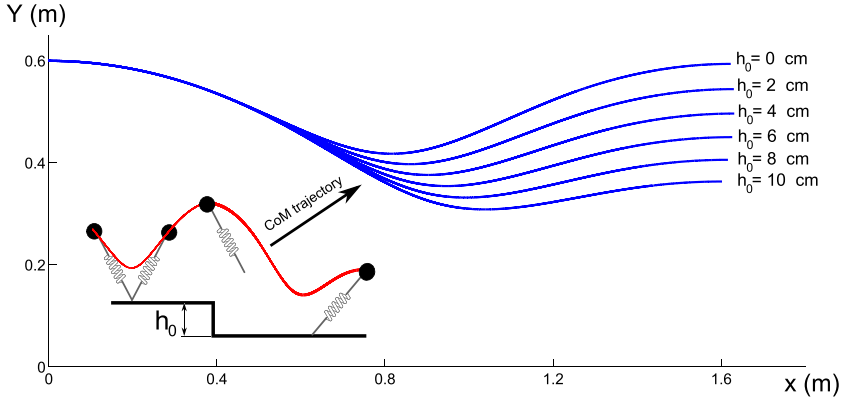

Figure 8. CoM trajectory trend of the system with different drop heights. In animals running, the same behavior for the CoM trajectory is observed [7].

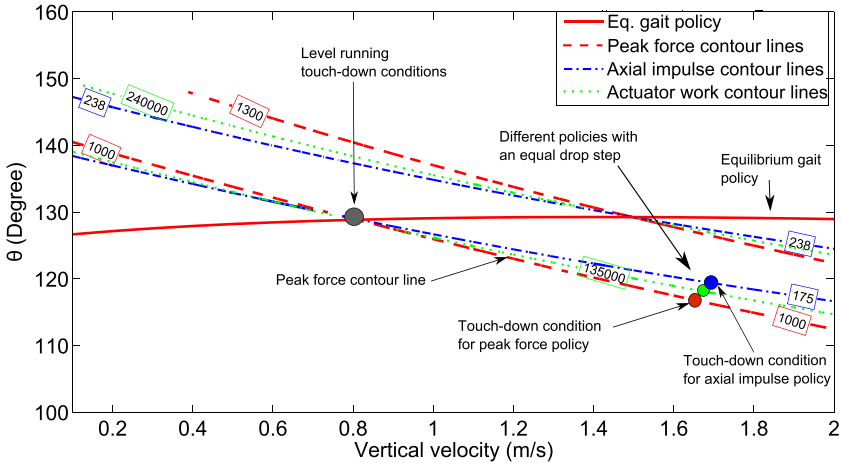

Figure 9. Contour lines for leg peak force (red), axial impulse(blue) and leg actuator electric work(green). The big gray circle shows the level running touch-down condition and the small colored circles show the touch-down angle at the drop step following each of the control policies. Since the contour lines are close to linear respect to vertical velocity (or time), a constant angular rate for the leg retraction would be a good approximation for the policies.

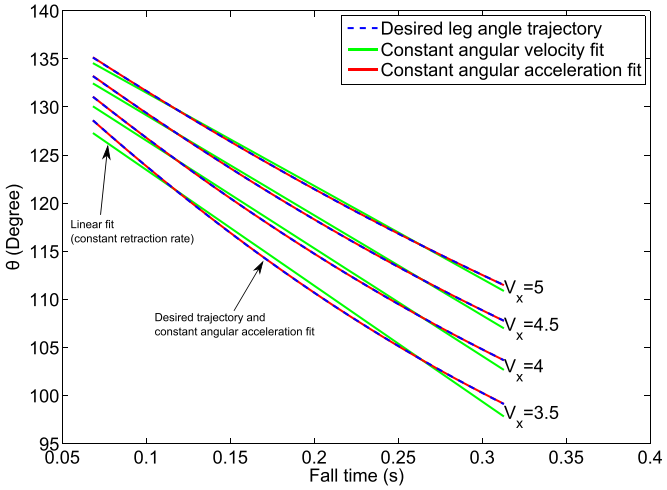

Figure 10. Desired and fit functions for the leg angle trajectory subjected to the constant peak force policy. The blue dashed lines are the desired leg angle trajectory and the green solid lines and red solid lines are linear and quadratic fit respectively. The constant angular acceleration fits the exact desired trajectory very well. As the forward speed increases, the constant retraction rate approaches the exact desired trajectory. The value for the retraction rate can be obtained from the slope of the contour lines.

increasing forward speed. The quadratic function, however, is an excellent fit for the leg angle trajectory.

5. Discussion

All three proposed control policies produce nearly identical leg angle trajectories, are clearly distinct from the equilibrium gait policy [12, 21], and successfully negotiate the drop step while achieving their specific objectives. The policies were hypothesized based on their relation to pragmatic locomotion goals such as safety and energy efficiency. They are mathematically related, and as such might be expected to generate similar behaviors; however, the spring-mass model can be sensitive to small policy changes, so it was unclear how they would relate to one another and the equilibrium gait when implemented. These results show that a single policy achieves both pragmatic locomotion goals of safety and efficiency at the same time.

Results show that the actuators require much more electrical energy in the drop step to maintain equilibrium gait than by using one of the proposed control policies. The 45% increase of the leg force may lead to serious structural damage to the leg, and even if the structure of the leg can sustain this new force, the motors and electronics may not be able to provide that much force and hence lead to falling. For the proposed control policies, on the other hand, the internal demands remain nearly the same as before. For example, the leg peak force increases only slightly (about 2−3%) for both constant impulse and constant work policy, and, of course, remains constant for the constant peak force policy. It should be noted that the electric energy that we consider here is to keep the leg motor locked and is due to the resistance of the electric motor. When there is need to do some mechanical work during the stance (which is not considered in this study), that work should be added to the resistance electric work.

The asymmetric shapes of the CoM trajectories resulting from the proposed control policies during the drop step imply that the robot accelerates horizontally in the drop step for all three proposed control policies. This is consistent with the behavior that animals show in the drop step [7]. However, with the equilibrium gait policy, the robot maintains the same forward speed during running. The increase of the horizontal velocity in the drop step for the proposed control policies is due to the conversion of potential energy (of the drop height) into kinetic energy. Since the velocity contributes quadratically to the kinetic energy, the resulting horizontal velocity does not increase significantly, especially for high forward speeds. For example, if the initial forward speed is 5 m s^{-1}, after redirecting the added potential energy from falling into a 20 cm drop into horizontal velocity, the resultant forward speed will be

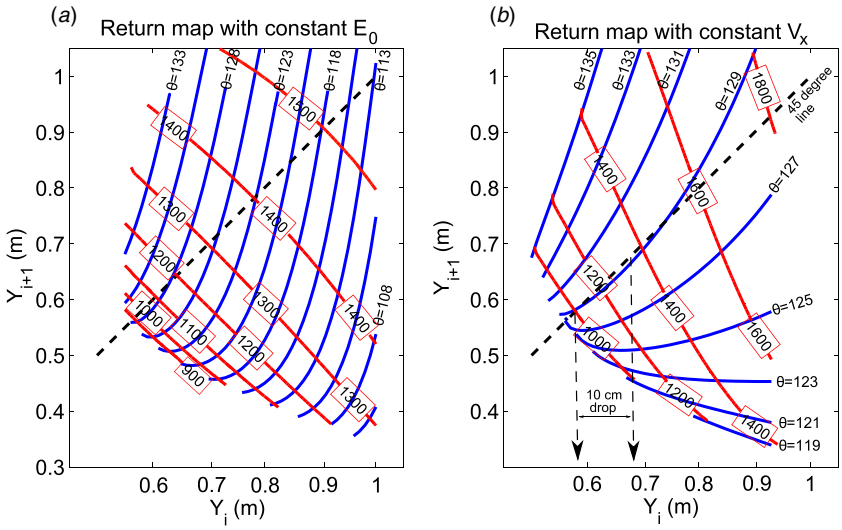

Figure 11. Return map with constant mechanical energy ([9, 12]) (*a*) and return map with constant horizontal velocity (*b*). There are two sets of contour lines: leg angle (θ) contour lines [degree] are in blue and axial peak force contour lines [N] are in red.

5.4 m s^{-1}. This means the forward speed increases only by 8% after falling from 20 cm height.

In this study, we focused on the mechanical and electrical limitations of the actuators that facilitate the control policies. Other preferred requirements like the next stride apex height and apex horizontal velocity are of second priority for the control policies and can be determined similar to the dead-beat control strategies [21, 33], or the Raibert controller [34].

Since the contour lines in the leg angle (θ)—fall time (t) plane (figure 9) are nearly linear, retracting the leg with a constant angular velocity, determined by the average slope of the contour lines, would be a simple implementation. The value for the leg retraction rate agrees with Karssen *et al* [22]. Further investigation of the contour lines reveals that leg retraction with a constant angular acceleration is a more accurate fit for the swing leg trajectory, but for high forward speeds (>6 m s^{-1}), the angular leg trajectory with constant angular velocity is close enough. To cover all speeds, however, the constant angular acceleration fit is the better choice.

The objective functions that we chose for the policies are of great technical importance from a roboticist's point of view. We tried to find an exact map that regulates our objective functions, but surprisingly the map function happened to be simply a constant leg angular acceleration. For short flight times (falling from small drop heights), constant leg angular velocity is a good approximation for this map. The outcomes agree with what Karssen *et al* [22] found for the optimal swing leg retraction rate when the peak force is considered as the objective function. But contrary to their work, we did not limit our policy to a constant leg retraction rate.

The difference between the proposed control policies and the equilibrium gait policy increases as the forward speed increases. To provide steady state running for high forward speeds, using an equilibrium gait controller, the leg should protract in the falling half of the flight phase (see appendix), but for all three proposed control policies the leg is retracted to reach the ground. The leg protraction in the equilibrium gait policy postpones the instant of touch-down and consequently increases the difference of the proposed control policies and the equilibrium gait policy. Karssen *et al* [22] also reported that the difference between optimal swing leg retraction rate for disturbance rejection and other objective functions (including the leg peak force) increases with increasing forward speed.

The desired leg angle trajectory for each of the proposed control policies is different with the two-phase constant leg retraction rate in the clock-driven model that was proposed for robots like RHex [1, 2, 35]. In each of our proposed control policies, as well as in the clock-driven model, after the time of the expected touch-down, the leg trajectory follows a different trajectory function. However, in the policies proposed here, instead of a constant retraction rate, a constant angular acceleration is applied to the leg. More importantly, contrary to the clock-driven method, the leg control stops at the beginning of stance phase (the three proposed control policies are purely passive in stance phase). The clock-driven method is a simple bio-inspired technique, but it does not consider the structural or electrical capacity of the leg, and may therefore lead to failure during stance.

By using a new type of return map, the proposed control policies and their limitations can be depicted visually. In this new type of return map, contrary to return maps with constant mechanical energy [9, 12] (figure 11(*a*)), the horizontal velocity is kept constant (figure 11(*b*)). In a return map with constant energy, any change in the ground level alters the energy of the system and therefore, flight phase control policies with varying ground level cannot be depicted on the map (figure 11(*a*)). In the return map that we use here, instead of the mechanical energy, the horizontal velocity is kept constant (figure 11(*b*)). The key difference of these two return maps is: the axes in the return map with constant mechanical energy represent the apex heights relative to the original ground level, but in the return map with constant forward speed, the two axes are the apex heights relative to the upcoming stance

phase ground level. In figure (11(*b*)), y_i represents the apex height relative to the upcoming stance phase. Therefore, any change in ground height is interpreted as the change in y_i (for example, if there is a 10 cm drop step, the apex height increases by 10 cm). The vertical axis of this graph (y_{i+1}) is the apex height relative to the upcoming stance ground level.

When the constant peak force control policy is implemented, the leg angle is adjusted such that its return map is parallel to the axial peak force contour lines. Using the constant forward speed for this map allows us to interpret the change of the ground level as a change in the apex height. Therefore, contrary to the conventional return map [9, 12], we do not need to change the graph. For example, if the apex height for steady state running is 57 cm then the peak force would be 1000 N. Now, we assume the drop height is 10 cm; therefore, the apex height including the drop step would be 67 cm. To follow the constant peak force policy, the leg angle should be set to $\theta = 121^\circ$ at the moment of touch-down, and the passive dynamics of the system will result in the same axial peak force as before (1000 N). It should be noted that there is no need to know the ground level in advance, since the leg angle is continuously being updated expecting to reach the ground any moment. To achieve steady state running (equilibrium gait), the controller should follow the 45° line, which requires the touch-down angle to be about $\theta = 129^\circ$. Consequently, the peak force in the leg increases to about 1350 N (35% increase). We also notice that although the constant peak force policy prevents the peak force from increasing, it has a limit for the maximum drop height that can be handled by this control policy. For example, to keep the peak force equal to 1000 N, the maximum drop height is 10 cm (the end of the 1000 N contour line). This implies that for deeper drops, the peak force has to increase to prevent the robot from falling or additional control inputs are required, such as a change in leg length.

Because of the negative slope of the force contour lines in the return map, the next apex height decreases with increasing drop height. This implies that the system gains horizontal velocity due to the transformation of potential energy into kinetic energy. This behavior is confirmed by simulations and can also be observed in animal experiments [7]. We know that for a successful running gait, the subsequent apex height is an important factor that also needs to be considered. The subsequent apex height after the drop step should be greater than a predefined threshold, and the flight phase should be long enough to allow the leg to be placed on the ground for the next stride. Therefore, based on the geometry of the leg, the negotiable drop height is limited by the controller. However, if the controller was allowed to change the leg length of the subsequent step, another option would be to continue running with a shorter leg length. For all these cases, the return map with constant horizontal velocity visualizes the limitations and can help designing an appropriate scenario for the control policy.

The findings of the return map that we presented for constant peak force policy, can be easily extended to axial impulse or leg work. In these cases, only the peak force contour lines in figure 11 would change to the impulse or leg work contour lines in the range of $175N.S$ –$300N.S$, and $135\,000N^2.S$–$350\,000N^2.S$, respectively. The overall shape of the impulse/leg work contour lines are similar to the peak force contour lines in figure 11.

It should be remembered that all three proposed control policies adjust the leg angle during flight, and the system is assumed to be conservative. Therefore, to continue running on ground with a permanent drop step, the robot should dissipate the gained kinetic energy. In this case, a stance phase control would be required to bring the robot back to the preferred forward speed, or the robot would continue with a higher horizontal velocity. A simple and bio-inspired stance phase technique that was proposed by Schmitt *et al* [36] and investigated more by [37] and [38] could be used to dissipate the gained energy. Since the energy that requires dissipation is only that due to the drop perturbation, the cost of dissipating this energy in subsequent steps is the same across all control policies compared. If the energy were dissipated within the perturbed step, this could lead to different energetics for different policies that require energy dissipation while meeting other mechanical objectives. The equilibrium gait policy requires high force, and the proposed control policies have relatively short stance periods, and these factors could influence the cost of dissipation depending on motor/muscle characteristics. By allowing the energy dissipation to occur in subsequent steps following the perturbation, the energy can be dissipated in the energetically optimal period of stance.

The simulations and the results presented in this work are designed for unexpected step-down disturbances in the ground level. For the case of step-up disturbances, since the touch-down occurs early, the vertical velocity of the CoM has not reachined its prior peak values, therefore an equilibrium gait can be obtained with lower values for the leg force or work (in section 5.1 it is explained more on the return map as well). The height of the step-up disturbance that can be handled depends on the length of the leg. To increase the control authority in handling the step-up disturbances (running over larger step-up disturbances), other scenarios (like shortening the leg length during the flight phase) can be used that are not in the scope of this study. As an example, during the first half of the flight phase (CoM going upward) the leg can be getting shortened (to provide enough space for the possible obstacles) and during the second half of the flight phase, as the leg length is being increased to its nominal length, the leg angle is adjusted accordingly to provide an equilibrium gait at the moment of contact with the leg length at that moment.

5.1. Stability analysis of the proposed control policies

In this section, we investigate the stability of the proposed control policies and compare them with the stability of the equilibrium gait policy. To give this comparison, we use the return map with constant energy level (figure 11) in more details for each case. More information about the return map with constant energy was presented earlier and can be found in [9, 10, 12]. For the conservative SLIP model, since the energy level is constant, the only variable of the system would be the apex height at each stride. Therefore, the perturbations in stability analysis are applied to the apex height while the

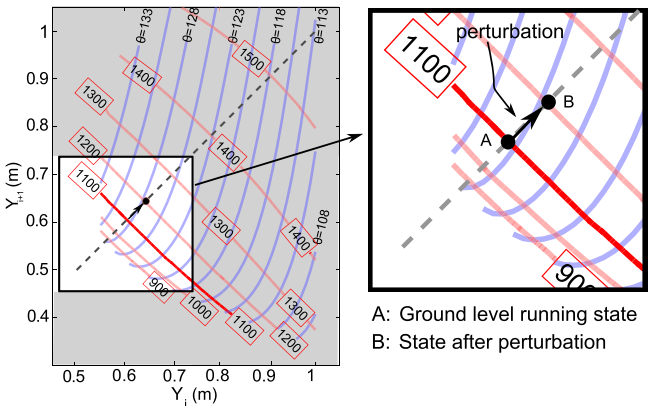

Figure 12. The return map with constant energy. After the perturbation, the location of the state changes from point A (ground level running) to the perturbed state on the 45° line (point B) and the system continue running in this state. It shows the neutral stability of the equilibrium gait policy. The red curves are leg peak force contour lines and the blue curves are touch-down angle contour lines.

whole energy of the system is kept constant. For more details about the stability analysis of the SLIP model running refer to [9, 11, 12, 39].

We first start with investigating the stability of the equilibrium gait policy. Figure 12 shows how the perturbation in the apex height changes the location of the states on the return map. The equilibrium gait policy controls the states to move along the 45° line to always have a symmetric trajectory. For example, if the level ground running is shown by point A in figure 12, after the perturbation, the system would be on state B along the 45° line. Since this policy always keeps the states on the 45° line, the next state has the same apex height as the perturbed state which implies neutral stability. Figure 13 shows the CoM trajectory of the perturbed and unperturbed systems with this control policy. Because of the neutral stability of the equilibrium gait policy, the perturbations do not vanish and the system continues running in the new symmetric trajectory.

Figure 14 shows the stability of the proposed control policies (constant peak force policy for example). Like before, we assume the system is running on the level ground at state A. After the perturbation, the apex height goes to state B_1 which has the same leg peak force (it moves along the peak force contour lines). For the next step, the system goes to state B_2 to keep the leg peak force constant and then returns back to state

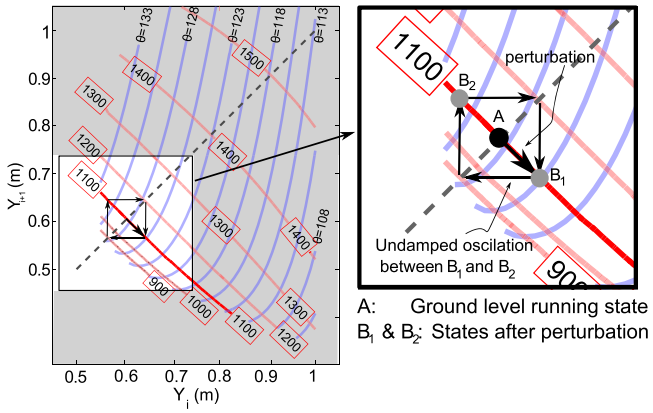

Figure 14. The return map for constant peak force policy. After the perturbation, the system oscillates between states B_1 and B_2.

B_1 and so on. The CoM trajectory of the system in this case is shown in figure 15. In this case, the CoM trajectory is periodic in two steps instead of one step in equilibrium gait policy and like equilibrium gait policy it has neutral stability.

Due to the negative slope of the leg peak force contour lines, the next apex height after the drop step is lower than the drop step apex height. It implies that after the drop step the system can continue in a new equilibrium gait with a lower leg peak force, impulse and leg work. The return map in this case is shown in figure 16. After the perturbation, the system goes from state A (ground level running) to state B_1 along the contour lines to retain the leg peak force. For the next step, the system can converge to state B (on the 45 ° line) which is an equilibrium state with lower leg peak force. The CoM trajectory of the system in this case is more compatible with the animals data encountering drop step perturbation. The CoM trajectory of the system under drop step-like perturbation (increased apex height) is shown in figure 17.

When the perturbation is like a step-up obstacle, the perturbed apex height is smaller than the level running, thus the peak leg forces are lower, and the resulting new equilibrium gait will satisfy peak force limits.

In summary, the proposed control policies, like equilibrium gait policy, converge to new CoM trajectory after the disturbance. When they are used with equilibrium gait policy for after the drop step, the system will continue with a new symmetric CoM trajectory. Assuming the robot keeps the gained energy level, the robot will continue running with a higher forward speed.

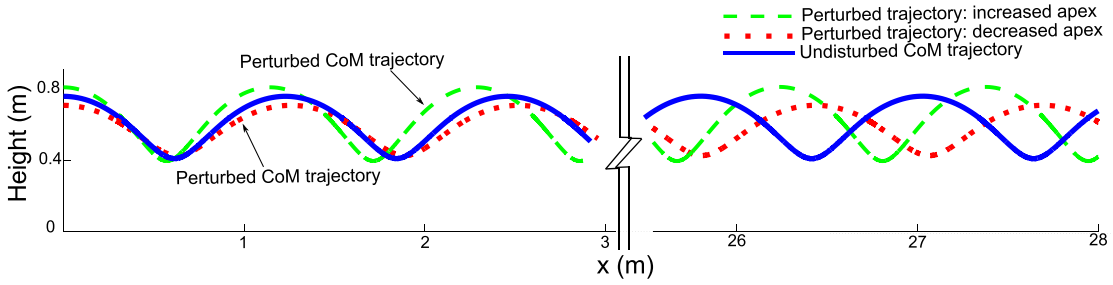

Figure 13. The CoM trajectory of the unperturbed and perturbed SLIP model with equilibrium gait policy. Because of the neutral stability of the equilibrium gait policy, the system remains in the perturbed state.

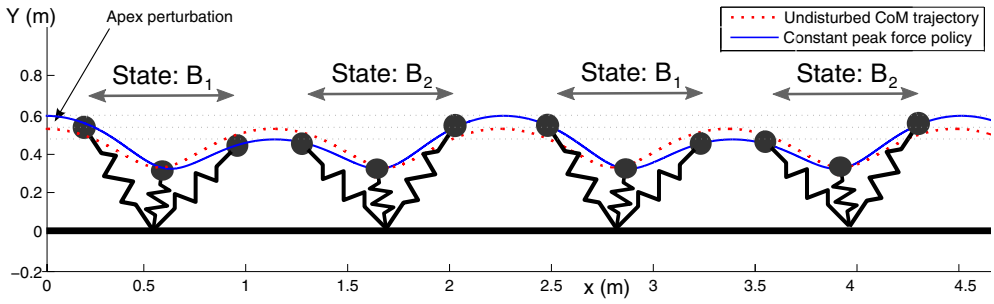

Figure 15. The CoM trajectory of the system going from state B_1 to state B_2 and return to B_1 and so on.

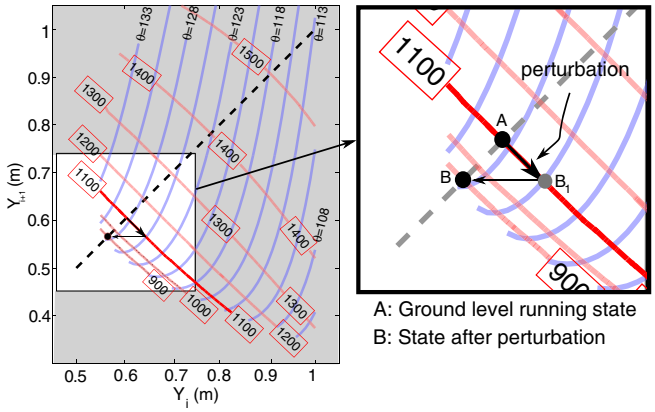

Figure 16. The return map with constant energy. After the perturbation, the system goes to state B_1 for one step and then using equilibrium gait policy, it stays at state B.

6. Conclusion and future work

Three flight phase control policies inspired by animal data, but suitable for machines, were proposed and implemented to the model of a spring-mass running robot. The control policies regulate their objective functions that target the mechanical/amperage limitation and electrical efficiency of the system. By using either of these bio-inspired control policies, the safety and efficiency of the robot during running is guaranteed, while their implementation is very easy with minimal sensing requirements.

All three proposed control policies (constant peak force, constant axial impulse and constant leg actuator electric work) successfully negotiated the drop step, and surprisingly resulted in similar behavior of the spring-mass robot. Therefore, by implementing either of these proposed control policies, both goals, damage avoidance and efficiency, would be satisfied.

We showed that a simple leg angular acceleration during the flight phase keeps running safe (avoiding the damage) and efficient. If the drop height is less than 10% of the leg length, a constant leg angular velocity (constant leg retraction rate) would lead to similar results. The value of the leg retraction rate (leg angular velocity) can be derived from the slopes of the leg peak force contour lines in the leg angle-falling time plane. It should be noted that implementing these policies is very easy because the constant angular acceleration for the leg can be provided by constant motor torque ($T = I \cdot \ddot{\theta}$) and since the relation between the motor torque and current is linear, therefore providing a constant current places the toe at the right location at each instant.

For future work we plan to implement these policies on our robot ATRIAS. We found that the amperage limitation is a big concern for electrically actuated spring-mass robots like ATRIAS, and therefore, we will start with the constant leg peak force policy.

Acknowledgments

This study was funded by grant RGY0062/2010 from the Human Frontier Science Program and grant 1100232 from the National Science Foundation.

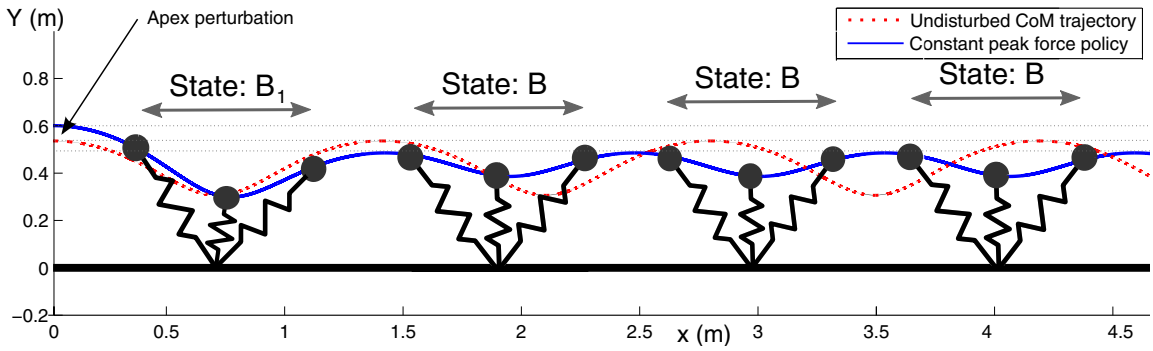

Figure 17. CoM trajectory of the perturbed and unperturbed system. After regulating the objective function (peak force here), the system goes through a transition state (B_1) and then stays at a state with lower peak force (B).

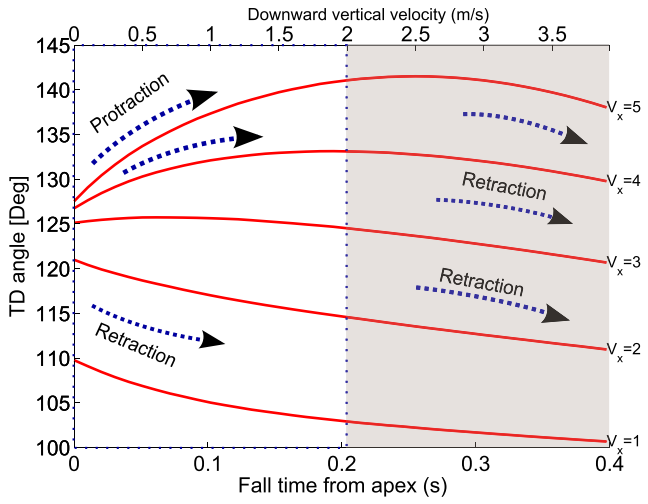

Figure A1. The required leg angle trajectory for equilibrium gait policy. For low horizontal velocities, the leg should be retracted as it falls. For high forward speeds (here about $v_x > 3$ m s^{-1}) the robot should protract the leg in the beginning and then it should start retracting the leg. The shaded area corresponds to deep drops (disturbances more than about 30% of the leg length that is not very common for legged robots to reject blindly.

Appendix. Equilibrium gait policy

The equilibrium gait policy ensures that the robot has symmetric CoM trajectories during stance with respect to the vertical axis defined by mid-stance (i.e. touch-down and take-off conditions are symmetrical). In previous work [7] we showed that even though for high forward speeds leg protraction is mathematically needed to keep equilibrium gait policy during running, guinea fowl always retract their legs in the presence of drop step and they never protract their legs during falling. To result in symmetric gait for high forward speeds in the presence of a drop, the leg should protract as the CoM falls in the drop (figure A1). This protraction opens more room between the toe and the ground, and consequently leads to higher vertical velocity at the time of touch-down. Figure A1 shows the leg angle trajectory with respect to falling time for different forward speeds that results in equilibrium gait. For low horizontal velocities, the leg angle function is monotonically decreasing, meaning that the leg should be retracted after apex. For high forward speeds (here $v_x > 3$) the robot should protract the leg in the beginning, and then (after gaining some downward velocity, and if it did not yet touch the ground) should start retracting the leg to provide the appropriate leg angle for equilibrium gait. For human-scale spring-mass running robots, high downward velocity (here more than about 2 m s^{-1}, which corresponds to a drop height of about 30% leg length) is not common to be rejected blindly. Therefore, for small to medium drops, the leg would have monotonic behavior. This is interpreted as retraction for low forward speeds, and protraction for high forward speeds as the robot falls.

Karssen *et al* [22] also concluded that for high horizontal velocities, the trade-off between disturbance rejection, energy loss, and foot slipping increases. On the one hand side, the leg should be protracted the reject disturbances, but on the other hand, the leg should be retracted to reduce impacts and prevent foot slipping. Moreover, as the robot falls, the protraction increases the distance between the toe and the ground and postpones the contact moment, meantime the vertical velocity increases, and consequently the leg peak force and axial impulse increase even more.

References

[1] Saranli U, Buehler M and Koditschek D E 2001 RHex: a simple and highly mobile hexapod robot *Int. J. Robot. Res.* **20** 616–31

[2] Altendorfer A, Moore N, Komsuoglu H, Buehler M, Brown H B Jr, McMordie D, Saranli U, Full R J and Koditschek D E 2001 Rhex: a biologically inspired hexapod runner *Auton. Robots* **11** 207–13

[3] Raibert M, Blankespoor K, Nelson G and Playter R and the BigDog Team 2008 Bigdog, the rough-terrain quadruped robot *IFAC'08: Proc. 17th World Congr. of the International Federation of Automatic Control (Seoul, Korea, 6–11 July)*

[4] Grizzle J W, Hurst J, Morris B, Park H W and Sreenath K 2009 MABEL, a new robotic bipedal walker and runner *ACC'09: Proc. Conf. on American Control Conference (St. Louis, USA, 10–12 June)*

[5] Grimes J and Hurst J 2012 The design of atrias 1.0 a unique monopod, hopping robot *CLAWAR'12: Proc. 15th Int. Conf. on Climbing and Walking Robots and the Support Technologies for Mobile Machines (Baltimore, MD, USA, 23–26 July)*

[6] Kuo A D 2007 Choosing your steps carefully *IEEE Robot. Autom. Mag.* **14** 18–29

[7] Blum Y, Vejdani H R, Birn-Jeffery A, Hubicki C, Hurst J and Daley M A 2013 Trade-off between disturbance rejection and injury avoidance in running guinea fowl *PloS One* (under review)

[8] Geyer H, Seyfarth A and Blickhan R 2006 Compliant leg behaviour explains basic dynamics of walking and running *Proc. R. Soc.* B **273** 2861–7

[9] Seyfarth A, Geyer H, Guenther M and Blickhan R 2002 A movement criterion for running *J. Biomech.* **35** 649–55

[10] Seyfarth A, Geyer H and Herr H 2003 Swing-leg retraction: a simple control model for stable running *J. Exp. Biol.* **206** 2547–55

[11] Blum Y, Lipfert S W, Rummel J and Seyfarth A 2010 Swing leg control in human running *Bioinspir. Biomim.* **5** 026006

[12] Ernst M, Geyer H and Blickhan R 2012 Extension and customization of self-stability control in compliant legged systems *Bioinspir. Biomim.* **7** 046002

[13] Moritz C T and Farley C T 2004 Passive dynamics change leg mechanics for an unexpected surface during human hopping *J. Appl. Physiol.* **97** 1313–22

[14] Daley M A, Voloshina A and Biewener A A 2009 The role of intrinsic muscle mechanics in the neuromuscular control of stable running in the guinea fowl *J. Physiol.* **587** 26932707

[15] Daley M A and Biewener A A 2011 Leg muscles that mediate stability: mechanics and control of two distal extensor muscles during obstacle negotiation in the guinea fowl *Phil. Trans. R. Soc.* B **366** 1580–91

[16] Birn-Jeffery A and Daley M A 2012 Birds achieve high robustness in uneven terrain through active control of landing conditions *J. Exp. Biol.* **215** 2117–27

[17] Daley M A and Biewener A A 2006 Running over rough terrain reveals limb control for intrinsic stability *Proc. Natl Acad. Sci. USA* **103** 15681–6

[18] Herr H M and McMahon T A 2001 A galloping horse model *Int. J. Robot. Res.* **20** 26–37
[19] Daley M A and Usherwood J R 2010 Two explanations for the compliant running paradox: reduced work of bouncing viscera and increased stability in uneven terrain *Biol. Lett.* **6** 418–21
[20] Blum Y, Birn-Jeffery A, Daley M A and Seyfarth A 2011 Does a crouched leg posture enhance running stability and robustness? *J. Theor. Biol.* **281** 97–106
[21] Ernst M, Geyer H and Blickhan R 2009 Spring-legged locomotion on uneven ground: a control approach to keep the running speed constant *Proc. Int. Conf. on Climbing and Walking Robots (Istanbul, Turkey)* pp 639–44
[22] Karssen J G D, Haberland M, Wisse M and Kim S 2011 The optimal swing-leg retraction rate for running *ICRA'11: IEEE Int. Conf. on Robotics and Automation* pp 4000–6
[23] Blickhan R 1989 The spring-mass model for running and hopping *J. Biomech.* **22** 1217–27
[24] McMahon T A and Cheng G C 1990 The mechanics of running: how does stiffness couple with speed? *J. Biomech.* **23** 65–78
[25] Full R J and Koditschek D E 1999 Templates and anchors: neuromechanical hypotheses of legged locomotion on land *J. Exp. Biol.* **202** 3325–32
[26] Farley C T and Gonzalez O 1996 Leg stiffness and stride frequency in human running *J. Biomech.* **29** 181–6
[27] Ferris D P, Louie M and Farley C T 1998 Running in the real world: adjusting leg stiffness for different surfaces *Proc. R. Soc.* B **265** 989–94
[28] Grimmer S, Ernst M, Günther M and Blickhan R 2008 Running on uneven ground: leg adjustment to vertical steps and self-stability *J. Exp. Biol.* **211** 2989–3000
[29] Blickhan R, Seyfarth A, Geyer H, Grimmer S, Wagner H and Gunther M 2007 Intelligence by mechanics *Phil. Trans. R. Soc.* A **365** 199–220
[30] Srinivasan M 2011 Fifteen observations on the structure of energy-minimizing gaits in many simple biped models *J. R. Soc. Interface* **8** 74–98
[31] Chevallereau C, Choi J H, Morris B, Westervelt E R and Grizzle J W 2007 *Feedback Control of Dynamic Bipedal Robot Locomotion* (Boca Raton, FL: CRC Press)
[32] Remy C D, Buffinton K and Siegwart R 2012 Comparison of cost functions for electrically driven running robots *ICRA'12: Proc. IEEE Int. Conf. on Robotics and Automation* pp 2343–50
[33] Seyfarth A and Geyer H 2002 Natural control of spring-like running: optimized self-stabilization *Proc. 5th Int. Conf. on Climbing and Walking Robots (London, UK)* pp 81–6
[34] Raibert M H 1986 *Legged Robots That Balance* (Cambridge, MA: MIT Press)
[35] Altendorfer A, Koditschek D E and Holmes P 2004 Stability analysis of a clock-driven rigid-body slip model for RHEX *Int. J. Robot. Res.* **23** 1001–12
[36] Schmitt J and Clark J 2009 Modeling posture-dependent leg actuation in sagittal plane locomotion *Bioinspir. Biomim.* **4** 17–33
[37] Miller B, Schmitt J and Clark J E 2012 Quantifying disturbance rejection of slip-like running systems *Int. J. Robot. Res.* **31** 573–87
[38] Andrews B, Miller B, Schmitt J and Clark J E 2011 Running over unknown rough terrain with a one-legged planar robot *Bioinspir. Biomim.* **6** 026009
[39] Geyer H, Seyfarth A and Blickhan R 2005 Spring-mass running: simple approximate solution and application to gait stability *J. Theor. Biol.* **232** 315–28